

# Globular cluster system and Milky Way properties revisited<sup>★</sup>

E. Bica<sup>1</sup>, C. Bonatto<sup>1</sup>, B. Barbuy<sup>2</sup>, and S. Ortolani<sup>3</sup>

<sup>1</sup> Universidade Federal do Rio Grande do Sul, Instituto de Física, CP 15051, Porto Alegre 91501-970, RS, Brazil  
e-mail: [bica;charles]@if.ufrgs.br

<sup>2</sup> Universidade de São Paulo, Dept. de Astronomia, Rua do Matão 1226, São Paulo 05508-090, Brazil  
e-mail: barbuy@astro.iag.usp.br

<sup>3</sup> Università di Padova, Dipartimento di Astronomia, Vicolo dell'Osservatorio 2, 35122 Padova, Italy  
e-mail: ortolani@pd.astro.it

Received 13 October 2005 / Accepted 28 November 2005

## ABSTRACT

**Aims.** Updated data of the 153 Galactic globular clusters are used to readdress fundamental parameters of the Milky Way, such as the distance of the Sun to the Galactic centre, the bulge and halo structural parameters, and cluster destruction rates.

**Methods.** We build a reduced sample that has been decontaminated of all the clusters younger than 10 Gyr and of those with retrograde orbits and/or evidence of relation to dwarf galaxies. The reduced sample contains 116 globular clusters that are tested for whether they were formed in the primordial collapse.

**Results.** The 33 metal-rich globular clusters ( $[Fe/H] \geq -0.75$ ) of the reduced sample basically extend to the Solar circle and are distributed over a region with the projected axial-ratios typical of an oblate spheroidal,  $\Delta x : \Delta y : \Delta z \approx 1.0 : 0.9 : 0.4$ . Those outside this region appear to be related to accretion. The 81 metal-poor globular clusters span a nearly spherical region of axial-ratios  $\approx 1.0 : 1.0 : 0.8$  extending from the central parts to the outer halo, although several clusters in the external region still require detailed studies to unravel their origin as accretion or collapse. A new estimate of the Sun's distance to the Galactic centre, based on the symmetries of the spatial distribution of 116 globular clusters, is provided with a considerably smaller uncertainty than in previous determinations using globular clusters,  $R_{\odot} = 7.2 \pm 0.3$  kpc. The metal-rich and metal-poor radial-density distributions flatten for  $R_{GC} \leq 2$  kpc and are represented well over the full Galactocentric distance range both by a power-law with a core-like term and Sérsic's law; at large distances they fall off as  $\sim R^{-3.9}$ .

**Conclusions.** Both metallicity components appear to have a common origin that is different from that of the dark matter halo. Structural similarities between the metal-rich and metal-poor radial distributions and the stellar halo are consistent with a scenario where part of the reduced sample was formed in the primordial collapse and part was accreted in an early period of merging. This applies to the bulge as well, suggesting an early merger affecting the central parts of the Galaxy. The present decontamination procedure is not sensitive to all accretions (especially prograde) during the first Gyr, since the observed radial density profiles still preserve traces of the earliest merger(s). We estimate that the present globular cluster population corresponds to  $\leq 23 \pm 6\%$  of the original one. The fact that the volume-density radial distributions of the metal-rich and metal-poor globular clusters of the reduced sample follow both a core-like power-law, and Sérsic's law indicates that we are dealing with spheroidal subsystems at all scales.

**Key words.** Galaxy: globular clusters: general – Galaxy: structure

## 1. Introduction

Globular clusters (GCs) are potential witnesses of the formation processes that gave rise to the Milky Way. Because of their long-lived nature, GCs formed in the initial phases of the Galaxy may preserve information in their structure and spatial distribution that is essential to probe these early conditions. In this sense, derivation of the present-day spatial distribution of GCs, as well as their physical properties, can be used to infer

much about the Galaxy formation and evolution processes and trace the geometry of the Galaxy better.

Early models suggest that the Galaxy formed as a consequence of a monolithic, dissipative collapse of a single massive, nearly-spherical spinning gas cloud (e.g. Eggen et al. 1962; Sandage 1990). Initial conditions of this collapse included low-metallicity gas and a nearly free-fall regime. This process should be reflected in the GC population as a homogeneity in certain parameters, such as orbital motions and a restricted age range. However, later work presented observational evidence that the present-day GC population results not only from the primordial collapse but also from merging and captures of smaller neighbouring galaxies early in the history of

<sup>★</sup> Table 1 is only available in electronic form at the CDS via anonymous ftp to cdsarc.u-strasbg.fr (130.79.128.5) or via <http://cdsweb.u-strasbg.fr/cgi-bin/qcat?J/A+A/450/105>

the Galaxy (Searle & Zinn 1978; Zinn 1980) or in more recent events such as the accretion and disruption of the Sagittarius dwarf spheroidal galaxy (Ibata et al. 1994, 1997). On theoretical grounds,  $N$ -body simulations (using standard cosmological conditions such as cold dark matter) suggest that the hierarchical merging of satellites might be the main building blocks of galaxy formation (Bellazzini et al. 2003).

Present-day data picture the region within  $\sim 10$  kpc (inner halo/bulge) as formed essentially by the primordial dissipative collapse (e.g. van den Bergh & Mackey 2005), while the region outside  $\sim 15$  kpc (outer halo) was formed by later infall and capture of smaller fragments (Searle & Zinn 1978; Zinn 1993). Mackey & Gilmore (2004) and Mackey & van den Bergh (2005) studied the properties of GCs by means of the horizontal-branch morphology, photometric, and structural parameters. They found significant differences among age/metallicity sub-groups. Mackey & Gilmore (2004) report that  $\sim 30\%$  of the Milky Way GCs have properties similar to those of the GCs in the LMC, SMC, Fornax, and Sagittarius dwarf spheroidal galaxies. This suggests that a significant fraction of the Galactic GC population, in particular outer halo ones, has an extragalactic origin.

Regardless of its origin, the Galaxy contains  $\sim 150$  GCs that are characterised by a bimodal metallicity distribution, and distances to the Galactic centre of up to  $\sim 150$  kpc. With respect to the metallicity vs. position relation, the metal-rich GCs used to be associated with a disk and the metal-poor ones with the halo (Kinman 1959; Zinn 1985; Armandroff 1989). More recently the metal-rich GCs have been found to characterise a bulge population (Minniti 1995; Barbuy et al. 1999; Coté 1999; van den Bergh 2000). Chemical enrichment models of the Galaxy, especially for the central parts (Matteucci & Romano 1999; Matteucci et al. 1999), predict that the formation of the bulge occurred from the same gas, but even faster than the inner halo.

Considerable efforts have been undertaken in the last  $\sim 15$  years to obtain fundamental parameters of globular clusters by means of accurate CCD colour–magnitude diagrams e.g. for the central parts of the Galaxy (Barbuy et al. 1998). Harris (1996), as updated<sup>1</sup> in 2003 (and references therein), compiled parameters of GCs that we adopt as the starting point for this work. Hereafter we refer to Harris’ database as H03.

Previous work has focused on the study of global properties and correlations among intrinsic parameters of the Galactic GC system, including the search for correlations with position in the Galaxy, e.g. Djorgovski & Meylan (1994), van den Bergh (2003), and Mackey & van den Bergh (2005).

The significant improvement in the observational GC data is in itself a reason for checking whether classically adopted values related to the early formation of the Galaxy and the GC system are still valid. In the present study we use an updated set of GC parameters, e.g. reddening, metallicity, distance from the Sun, age, and orbital motion to address their spatial distribution. Since one of the latest derivations of the Galactic centre’s distance using GCs was made by Reid (1993), we also discuss that value now based on the updated GC data.

Our basic approach is to decontaminate the GC sample of the clusters that are clearly not related to the primordial collapse of the Galaxy. We do this by identifying young GCs, those with retrograde orbits and/or those related to the accretion of dwarf satellite galaxies.

This paper is organised as follows. In Sect. 2 we present the updated GC sample and isolate the clusters probably associated to the primordial collapse. In Sect. 3 we present projections of their positions onto the  $(x, y)$ ,  $(x, z)$ , and  $(y, z)$  planes, derive the distance to the Galactic centre and draw conclusions about Galactic structure. In Sect. 4 we build GC radial density profiles, fit them with different analytical functions, and discuss GC destruction rates. In Sect. 5 we discuss a possible scenario to account for the present spatial distribution of GCs. Concluding remarks are given in Sect. 6.

## 2. The updated globular cluster data set

In the last 10 years new entries have been added to the census of Galactic GCs either by means of discoveries or by identifications of misclassified open clusters, e.g. IC 1257 (Harris et al. 1997), ESO 280-SC06 (Ortolani et al. 2000), 2MASS-GC01 and GC02 (Hurt et al. 2000), GLIMPSE-C01 (Kobulnicky et al. 2005), the diffuse cluster-type object SDSSJ1049 + 5103 (Willman et al. 2005), and the recently re-classified GC Whiting 1 (Carraro 2005). For new and already known GCs, H03 has provided constant updating of fundamental parameters.

Parameters of the 153 presently known GCs in the Galaxy are listed in Table 1. We complemented the H03 database by adding information on new GCs in the last 2 years as indicated in the notes to Table 1. The presently updated GC data set will hereafter be referred to as the GC05 sample.

To estimate errors in distance determinations for the subsequent analyses, we took into account both GC05 and typical distance errors in the literature, which are dominated by reddening uncertainties (e.g. Barbuy et al. 1998). We adopt the following values for the reddening and distance error relation:  $\varepsilon = 0.05$  for  $E(B - V) \leq 0.2$ ,  $\varepsilon = 0.10$  for  $0.2 < E(B - V) \leq 0.8$ ,  $\varepsilon = 0.15$  for  $0.8 < E(B - V) \leq 1.5$ ,  $\varepsilon = 0.2$  for  $1.5 < E(B - V) \leq 2.0$ , and  $\varepsilon = 0.25$  for  $E(B - V) \geq 2.0$ , where  $\varepsilon$  is the fractional error in distance. Uncertainties in related parameters are obtained by propagation of  $\varepsilon$ .

As discussed in Sect. 1, the Galactic GC system is not expected to be homogeneous in terms of cluster origin. Since we intend to base our analysis on GCs with a high probability of formation in the primordial collapse, we exclude from GC05 those with evidence either of extragalactic origin or formation later than the collapse. To this category belong the GCs with retrograde orbits (e.g. Dinescu et al. 1999), ages younger than 10 Gyr (e.g. Salaris & Weiss 2002), direct relation or tidal debris of dwarf galaxies (e.g. Forbes et al. 2004), and finally, luminous GCs with evidence of being accreted dwarf galaxy nuclei (e.g. Mackey & van den Bergh 2005). References are given in Col. 12 of Table 1. We found that 37 GCs (24% of GC05) fit into one or more of these categories. The remaining 116 GCs are part of what we define hereafter as the reduced sample (RS-GC05). One caveat with respect to the

<sup>1</sup> At <http://physun.physics.mcmaster.ca/Globular.html>

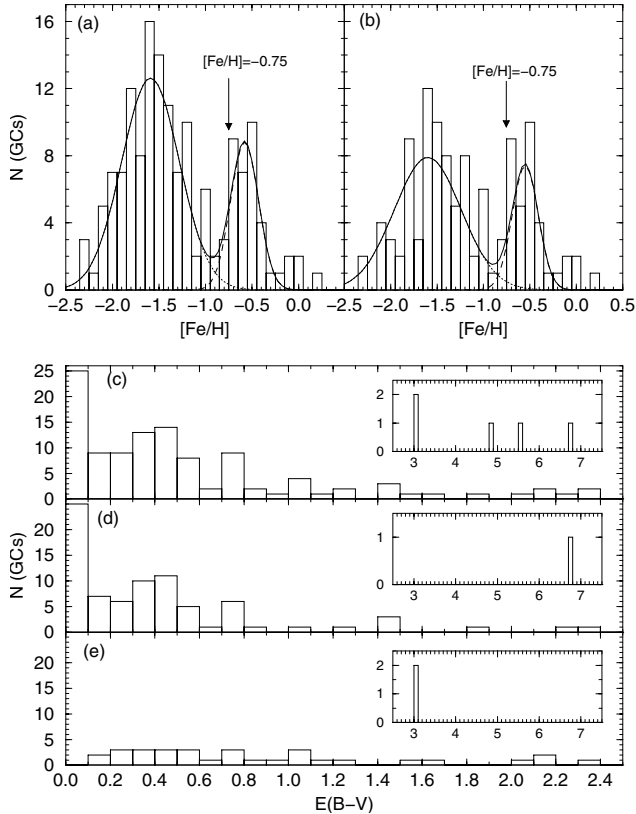


**Fig. 1.** The GC metallicity distribution of the GC05 (panel **a**) and reduced samples (panel **b**). The adopted threshold between metal-rich and metal-poor GCs is indicated. The reddening distribution of the reduced sample GCs is in panel **c**, the corresponding metal-poor ones are in panel **d**, and the metal-rich ones in panel **e**. The insets in panels **c**–**e** show the high-reddening range. Note that the two GCs with  $E(B - V) \approx 4.8$  and  $5.5$  (inset of panel **c**) have no metallicity determinations.

decontamination process is that it certainly is not sensitive to all events, accretions in particular, dating back to the first Gyr of the Galaxy. For instance, extragalactic GCs accreted in this period with prograde orbits would hardly be distinguishable in the present from the Milky Way’s native population.

Table 1 contains, by columns: (1) – the main GC designation; (2) and (3) – Galactic coordinates; (4) – reddening; (5) – metallicity; (6) – distance from the Sun; (7) – input Galactocentric distance; (8) – output Galactocentric distance (Sect. 3.1); (9)–(11) – input Heliocentric components (Sect. 3); (12) – indicators of non-collapse membership; and (13) – additional GC designations as compiled from the literature by one of us (E.B.).

In Fig. 1 (upper panels) we compare the globular clusters of RS-GC05 with those in GC05 in terms of metallicity. The well-known bimodal distribution in metallicity (seen e.g. as early as in Zinn 1985) is confirmed not only in the present GC05 sample (panel a) but also in RS-GC05 (panel b), although with a smaller amplitude ratio between the metal-rich and metal-poor GCs. In the subsequent analysis we adopt  $[\text{Fe}/\text{H}] = -0.75$  as the metallicity threshold between metal-rich and

metal-poor<sup>2</sup> GCs. RS-GC05 contains 81 metal-poor GCs, 33 metal-rich, and 2 with unknown metallicity (2MASS-GC02 and GLIMPSE-C01). The reddening distribution of the RS-GC05 GCs (panel c) is compared to those of the corresponding metal-poor (panel d) and metal-rich GCs (panel e). The reddening distribution of the metal-poor GCs presents a maximum around  $E(B - V) \approx 0.05$  and a smaller one at  $E(B - V) \approx 0.45$ . The low-reddening values are mostly related to halo GCs, while the high-reddening ones belong to a more central metal-poor component that spatially coexists with the metal-rich bulge clusters (Barbuy et al. 1998). The metal-rich GCs, in contrast, present a rather uniform distribution in the range  $0.05 \leq E(B - V) \leq 1.3$ .

### 3. Galactic structure and the distance to the centre

Inferences on the geometry of the GC system can be made by means of cluster positions projected onto the  $(x, y, z)$ -heliocentric coordinate axes (Table 1). In this coordinate system the  $x$ -direction increases from the Sun towards the Galactic centre,  $y$  is positive for  $\ell = 0^\circ - 180^\circ$  and  $z$  increases towards the north Galactic pole. We consider the metal-rich and metal-poor GCs separately, both of the GC05 and RS-GC05 samples. In Fig. 2 we show the positions of the metal-rich GCs projected onto the  $(x, y)$ ,  $(x, z)$ , and  $(y, z)$  planes for the GC05 (left panels) and RS-GC05 (right panels) samples. Because the  $(x, y, z)$  coordinates are in the heliocentric system, the centroids of the  $y$  and  $z$  distributions coincide with the Galactic centre, while that of the  $x$ -coordinate is shifted from  $x = 0$  (Sect. 3.1). The GC05 metal-poor and metal-rich GCs are more widely distributed than those in RS-GC05. This effect is minimised in the RS-GC05 plots because most of the GC05 outliers belong e.g. to accreted dwarfs or their debris and have young ages and/or retrograde orbits (Table 1). The 2 remaining outliers in the metal-rich RS-GC05 (panels b, d, and f), NGC 6356 and Palomar 11, basically define the outer limits of the metal-rich system, slightly beyond the present determination of the Solar circle (see below) – 8 kpc (Reid 1993). These clusters deserve further attention to clarify whether they are young GCs, thus not related to the collapse, and/or are located in the apogalacticon of their orbits.

From the plots involving the RS-GC05 sample (Fig. 2) we estimate that the metal-rich GCs distribute essentially in a region with dimensions  $\Delta x \approx 12$  kpc,  $\Delta y \approx 11$  kpc and  $\Delta z \approx 5$  kpc, corresponding to axial-ratios  $\Delta x : \Delta y : \Delta z \approx 1.0 : 0.9 : 0.4$ . These axial-ratios can be accounted for by an oblate spheroid with  $\sim 5.5$  kpc in radius and  $\sim 2.5$  kpc in height, a structure spatially coincident with the bulge. As compared to earlier studies, the present  $x$  and  $y$  distributions of the metal-rich GCs are similar in extent (Fig. 2) because of the minimisation of observational errors achieved with present-day data.

The metal-poor GCs of RS-GC05 are mostly contained in a region with dimensions  $\Delta x \approx 35$  kpc,  $\Delta y \approx 36$  kpc, and  $\Delta z \approx 30$  kpc, with axial-ratios  $\approx 1.0 : 1.0 : 0.8$ . Considering uncertainties, these axial ratios describe a slightly flattened sphere that reaches into the outer halo.

<sup>2</sup> For simplicity we refer to metal-poor GCs as the genuine together with the intermediate-metallicity ones.

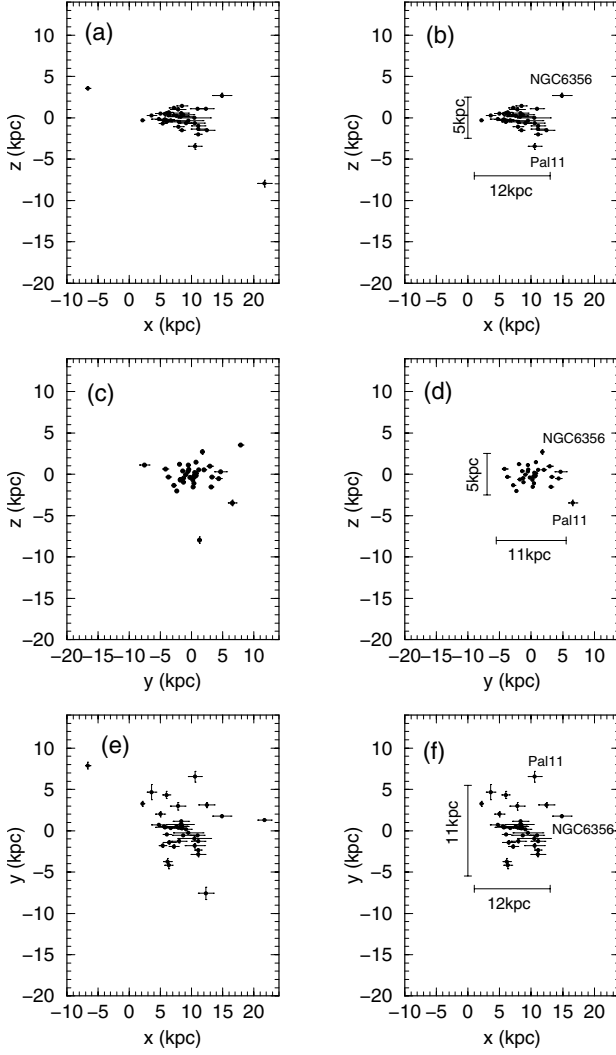


**Fig. 2.** Spatial projections of the heliocentric positions of the metal-rich GCs of the GC05 (*left panels*) and reduced (*right panels*) samples. The reduced sample produces more concentrated distributions. The outlier metal-rich GCs NGC 6356 and Palomar 11 are identified in panels **b**), **d**) and **f**).

We also infer the spatial distribution of the GCs in RS-GC05 by means of the distribution function  $\phi(\xi) = \frac{dN}{d\xi}$ , which counts the number of GCs in bins of  $\Delta\xi = 1$  kpc, for the  $x$ ,  $y$ , and  $z$  coordinates. According to the definition,  $\phi(\xi)$  is related to the projected one-dimensional number-density of GCs in a given direction. Figure 4 shows the distribution functions of all GCs in RS-GC05, and the corresponding metal-poor and metal-rich ones, separately. As expected from Figs. 2 and 3, the distribution functions in  $y$  and  $z$  are symmetrical with respect to the centroid of the coordinate system (the Galactic centre), while the shift in  $x$  provides the distance of the Sun to the Galactic centre (Sect. 3.1). The distribution functions in Fig. 4 can be fitted both with exponential-decay and squared-hyperbolic secant functions. Exponential-decay functions usually describe projected surface-density profiles in spiral galaxy disks (Binney & Tremaine 1987), while self-gravitating isothermal models, such as the squared-hyperbolic secant, have been used in edge-on disks (e.g. Rice et al. 1996)

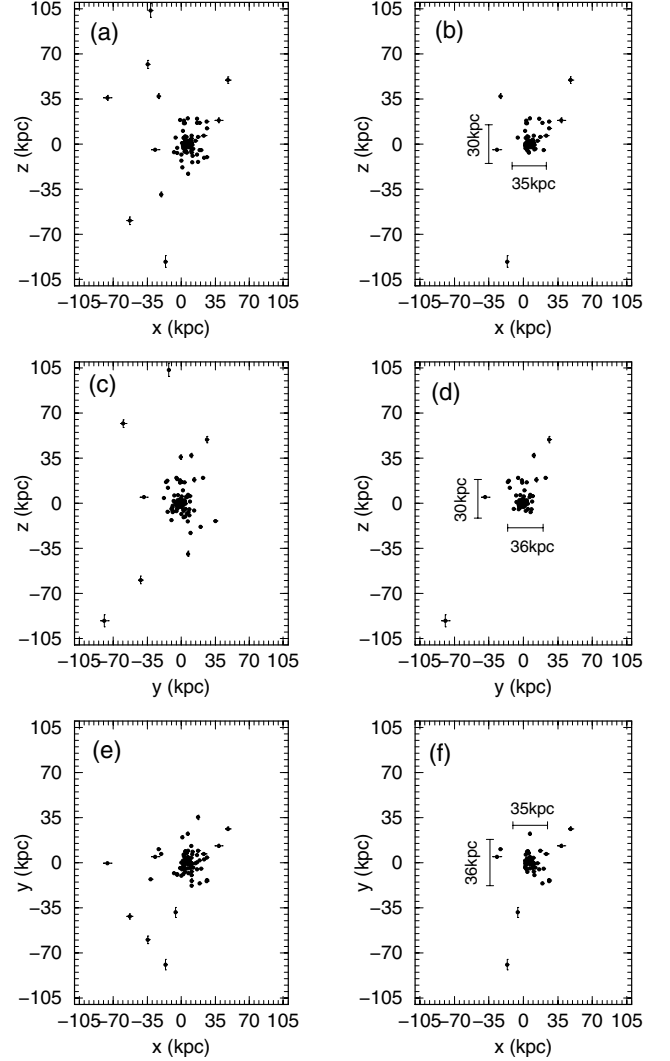


**Fig. 3.** Same as Fig. 2 for the metal-poor GCs.

and lenticular galaxies (van der Kruit & Searle 1981). Our purpose in fitting the distribution functions with a symmetrical profile is to derive the distance of the Sun to the Galactic centre (Sect. 3.1). In this sense we adopted the exponential-decay function  $\phi(\xi) \propto e^{-|\frac{\xi-\xi_0}{\xi_h}|}$ , since the respective correlation coefficients turned out larger than with squared-hyperbolic secant functions. The fits are shown in Fig. 4, and the resulting central positions ( $\xi_0$ ) and scale-lengths ( $\xi_h$ ) are given in Table 2. The distribution peaks in  $y$  and  $z$  occur, within uncertainties, at  $y = z = 0$  (Table 2 and Fig. 4).

Except for the central point in the  $y$ -distributions of the RS-GC05 sample (panel b) and corresponding metal-poor GCs (panel e), the exponential-decay function acceptably fits the observed data for distances of up to  $\sim \pm 7$  kpc with respect to the peak, within uncertainties. At such distances we are probing not only the bulge but also the inner halo. The fits preserve the symmetrical character of the observed profiles, and do not affect the centroid determination. This suggests that not many GCs remain undetected towards the central parts, at least to the point of affecting the distance determination.

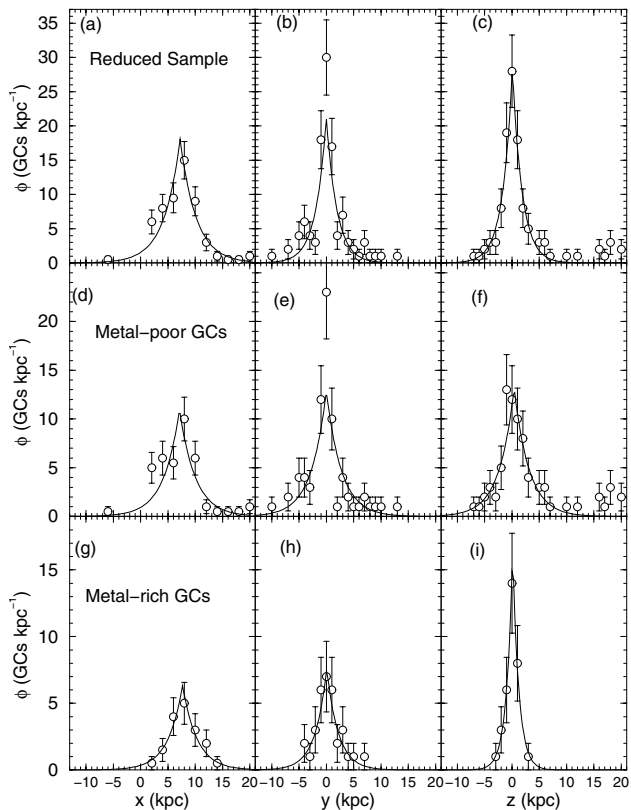


**Fig. 4.** One-dimensional distribution functions of the reduced sample (*top panels*), metal-poor (*middle panels*), and metal-rich GCs (*bottom panels*). The profiles were fitted with the exponential-decay function  $\phi(\xi) \propto e^{-|\frac{\xi-\xi_0}{\xi_h}|}$ .

**Table 2.** Parameters of the one-dimensional distributions.

(1)	Reduced sample GCs		
	All (2)	Metal-poor (3)	Metal-rich (4)
$x_0$ (kpc)	$7.2 \pm 0.3$	$7.1 \pm 0.5$	$7.7 \pm 0.3$
$x_h$ (kpc)	$2.9 \pm 0.4$	$2.9 \pm 0.6$	$2.7 \pm 0.4$
$y_0$ (kpc)	$0.0 \pm 0.3$	$0.0 \pm 0.4$	$0.1 \pm 0.3$
$y_h$ (kpc)	$1.9 \pm 0.4$	$2.8 \pm 0.5$	$2.1 \pm 0.4$
$z_0$ (kpc)	$0.1 \pm 0.2$	$0.4 \pm 0.3$	$0.1 \pm 0.1$
$z_h$ (kpc)	$1.8 \pm 0.2$	$2.7 \pm 0.5$	$1.1 \pm 0.1$
$x_h/y_h$	$1.5 \pm 0.4$	$1.0 \pm 0.3$	$1.3 \pm 0.3$
$x_h/z_h$	$1.6 \pm 0.3$	$1.1 \pm 0.3$	$2.4 \pm 0.4$
$y_h/z_h$	$1.1 \pm 0.3$	$1.0 \pm 0.2$	$1.9 \pm 0.4$

Notes. Parameters of the function  $\phi(\xi) \propto e^{-|\frac{\xi-\xi_0}{\xi_h}|}$  fitted to the  $\xi = (x, y, z)$  distribution functions. Column (2): all GCs of the reduced sample.

The individual fit of an exponential-decay profile to each of the  $(x, y, z)$  components does not necessarily imply a disk structure for the GC subsystems, since we are dealing with one-dimensional distribution functions and not surface density profiles.

The scale-length ratios (Table 2) derived from the exponential-decay fits agree, within uncertainties, with the

axial-ratios estimated from Figs. 2 and 3, both for the metal-poor and metal-rich GCs of RS-GC05.

### 3.1. Distance to the Galactic centre

The distance of the Sun to the Galactic centre ( $R_0$ ) has been a recurrent topic in the literature since Shapley's attempt in 1918 to derive it with globular clusters that resulted in  $R_0 = 13$  kpc. Since then different methods with more accurate data and larger GC samples have been used for the same purpose. For instance Frenk & White (1982) derived  $R_0 = 6.8 \pm 0.8$  kpc using a sample of 65 metal-poor and 11 metal-rich GCs limited in latitude to avoid exceedingly large reddening errors affecting distances.

Reid (1993) reviewed several estimators to derive  $R_0$ , among them the available GC parameters at that time. Estimates based on those GCs put  $R_0$  in the range 6.2–10.1 kpc. The average  $R_0$  from the GC determinations in Table 2 of Reid (1993) is  $7.9 \pm 1.4$  kpc, which coincides with his best value of  $8.0 \pm 0.5$  kpc considering all methods, e.g. calibration by OB stars and H I and H II regions, GCs, RR Lyrae, and red giants, among others. Since then this value has been widely employed in the literature. However, it is clear from his Fig. 3 that the  $x$  coordinates of the available GCs suffer from reddening/distance uncertainty effects. With the GC samples available at the time Maciel (1993) and Rastorguev et al. (1994) obtained  $R_0 \approx 7.6$  kpc and  $R_0 \approx 7.0$  kpc, respectively.

More recently, Eisenhauer et al. (2003) used VLT spectroscopic observations of the orbit of the star S2 around SgrA\* (assumed to be at the very centre of the Galaxy) to derive  $R_0 = 8.0 \pm 0.4$  kpc. In the same work they also provide the value of  $R_0$  based on the statistical parallax distance of 106 late-type and 27 early-type stars located in the central 0.5 pc. They obtained  $R_0 = 7.2 \pm 0.9$  kpc.

One caveat is that the total-to-selective absorption ratio  $R_V = A_V/E(B-V)$  is not expected to be uniform. Variations of  $R_V$  in different directions throughout the Galaxy can occur (e.g. Sumi 2004; Ducati et al. 2003).  $R_V$  is also affected by the effective wavelength shift in the filters owing to metallicity differences and reddening amount (Barbuy et al. 1998, and references therein). Detailed analyses of  $R_V$  in the directions of all GCs would be necessary to minimise  $R_V$ -related uncertainties. However, to a first approximation we assumed the H03 distances in Table 1, who took into account the metallicity dependence of the absolute magnitude of the horizontal branch; and from their data it can be inferred that a constant value of  $R_V = 3.1$  was adopted throughout.

At the  $1\sigma$  level the values of  $R_0$  provided by the one-dimensional exponential-decay fits of the metal-poor (panel d of Fig. 4) and metal-rich GCs (panel g) are basically the same (Table 2). In this sense, to increase the statistical significance of the determination we applied the fit to the 116 GCs of RS-GC05 (panel a of Fig. 4). We obtained an average value of  $R_0 = 7.2 \pm 0.3$  kpc. This value puts the Sun  $\approx 0.8$  kpc closer to the Galactic centre than either the best one adopted by Reid (1993) or the one derived by Eisenhauer et al. (2003). However, the present value coincides with that for central stars by Eisenhauer et al. (2003).

The present determination is based on a more accurate and numerous GC database, and consequently, the uncertainties in the value of  $R_O$  are a factor of  $\sim 3$  smaller than in previous studies using GCs (see Table 2 of Reid 1993). We used the new  $R_O$  determination to recalculate the Galactocentric distances (Col. 8 of Table 1).

### 3.1.1. Variable total-to-selective absorption

Following the analysis of Barbuy et al. (1998) of the central Galaxy, we now explore the effect of a varying total-to-selective absorption as a function of metallicity and reddening amount for the whole GC system. Following Grebel & Roberts (1995), we adopted  $R_V = 3.6$  for the GCs with metallicity higher than solar, and  $R_V = 3.1$  for  $[\text{Fe}/\text{H}] \leq -1.0$ . Interpolation is used for intermediate values of metallicity. To the metallicity-interpolated  $R_V$  we add a further correction related to reddening,  $\Delta R_V = 0.05 \times E(B - V)$  (Olson 1975). Dependence of distance on varying  $R_V$  can be expressed as

$$R'_O = R_O \times 10^{\frac{(R_V - R'_V)E(B-V)}{5}}.$$

We applied the above corrections to the data in Table 1 for all metal-rich GCs of RS-GC05 individually, leading to a lower value of  $R_O = 6.6 \pm 0.5$  kpc. Applying the same to all metal-poor GCs of RS-GC05 individually, the distance of the Sun to the Galactic centre remains essentially the same as before  $R_O = 7.3 \pm 0.5$  kpc (Table 2).

Finally, we considered the ensemble of the metal-rich GCs (Fig. 1) in order to minimise individual uncertainties. The average metallicity and reddening are  $[\text{Fe}/\text{H}] \approx -0.55$  and  $E(B - V) \approx 0.5$ , providing an average  $R'_V = 3.35$ . For the metal-rich GCs  $R_V = 3.1$  (Sect. 3.1) and  $R_O = 7.7 \pm 0.5$  kpc (Table 2), the resulting distance is  $R'_O = 7.3 \pm 0.3$  kpc, thus fully compatible with  $R_O$  derived from the metal-poor GCs.

Irrespective of the metallicity and reddening-law variations for the metal-rich GCs, the present distance of the Sun to the Galactic centre determination  $R_O \approx 7.2$  kpc is robust, since it depends mainly on the larger sample of metal-poor GCs. This is due to the metal-poor GCs being rather insensitive to  $R_V$  assumptions and the fact that the current accuracy on their distances is significantly improved.

## 4. Radial distribution of globular clusters

The distribution in Galactocentric distance of the GC number-density,  $\rho(R) = \frac{dN}{dV} = \frac{dN}{4\pi R^2 dR}$ , is a potential source of information not only on the present-day Galactic structure but also on the formation processes as well. To investigate this we built radial distribution profiles for the metal-rich and metal-poor GCs of RS-GC05 separately. Bins with a radius of  $\Delta R = 0.5$  kpc for  $R_{GC} \leq 10$  kpc are used to sample the inner regions better, while  $\Delta R = 2$  kpc for  $10 \leq R_{GC}(\text{kpc}) \leq 20$  and  $\Delta R = 10$  kpc for  $R_{GC} \geq 20$  kpc to avoid undersampling with increasing Galactocentric distance. Taken at face value, the radial distribution function as defined above should be applied to spherically symmetric systems, which is not the case of the oblate geometry of the metal-rich GCs of RS-GC05 (Sect. 3). Implications of this difference in geometry will be discussed in Sect. 4.4.

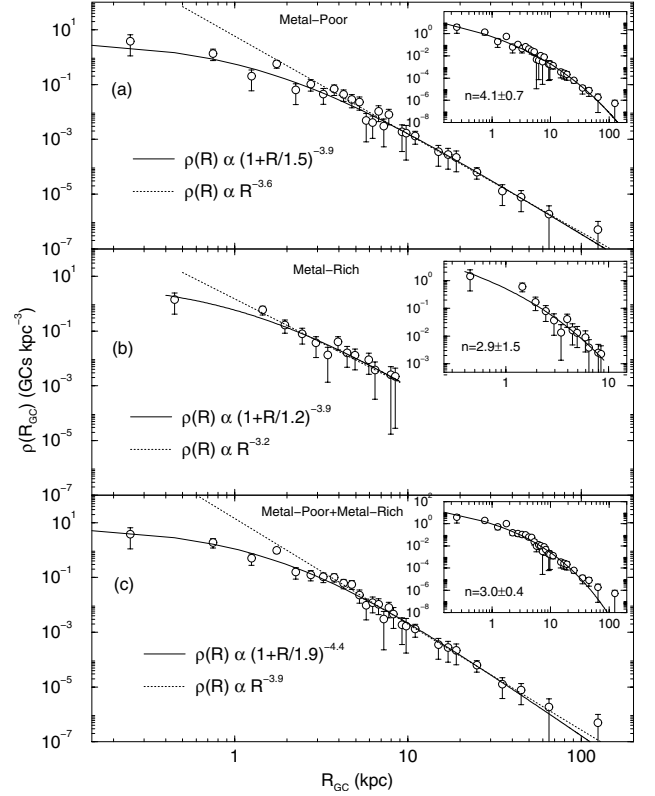


**Fig. 5.** Radial density profiles of the GCs in the reduced sample as a function of Galactocentric distance. Panel **a)** – metal-poor GCs; panel **b)** – metal-rich; panel **c)** – all GCs. Dashed line: single power-law fit for large Galactocentric distances. Solid line: fit of  $\rho(R) = \rho_o / (1 + R/R_C)^\alpha$ . Insets: fit of Sérsic’s law  $\rho(R) = a e^{-b[(R/R_C)^{1/m} - 1]}$ .

### 4.1. Metal-poor GCs

The radial distribution of the metal-poor GCs of RS-GC05 is shown in panel a) of Fig. 5. A fraction of 74% of the 81 metal-poor GCs is located at Galactocentric distances  $R_{GC} \leq 10$  kpc, and 20% at  $R_{GC} \geq 15$  kpc (outer halo). The distribution falls off smoothly as a rather steep power-law  $\sim R^{-(3.6 \pm 0.2)}$  for  $R_{GC} \geq 3.5$  kpc. However, it flattens out for smaller Galactocentric distances as  $\sim R^{-(1.7 \pm 0.3)}$ . At least part of the flattening might be attributed to completeness effects in the crowded central region of the Galaxy. However, a near-IR survey with 2MASS (Dutra & Bica 2000) did not reveal any new GC in the central region. Two recent GC discoveries with 2MASS are not centrally located, since they are at  $l \approx 10^\circ$  and near the plane, about halfway from the Sun to the Galactic centre (Hurt et al. 2000). Alternatively, the flattening for small  $R_{GC}$  may result from the cumulative destruction of GCs close to the Galactic centre over a Hubble time (a process that certainly played a major rôle in depleting the original GC population – see Sect. 4.5), or it may be an intrinsic feature of the radial distribution. Modelling of the spatial distribution of the old halo GCs beginning at the primordial collapse with cold baryonic gas and dark matter conditions suggests that the inner flattening may result not only from tidal destruction, but may in part have a primordial origin (Parmentier & Grebel 2005).

Because of the flattening at small  $R_{GC}$ , the simplest fits of the observed radial density profile are obtained with analytical functions that contain a core-like term. Following Djorgovski & Meylan (1994) we employ the function  $\rho(R) = \rho_0/(1 + R/R_C)^\alpha$ , where  $R_C$  is the core-like radius. We will refer to this function as the composed power-law. The agreement between fit and observed radial distribution along the full Galactocentric distance range is excellent (Fig. 5, panel a). The resulting parameters are  $\rho_0 = 3.9 \pm 2.5 \text{ kpc}^{-3}$ ,  $R_C = 1.5 \pm 0.6 \text{ kpc}$ , and  $\alpha = 3.9 \pm 0.3$ , with a correlation coefficient  $CC = 0.88$ .

Alternatively, in the inset of panel a we fitted the metal-poor observed radial profile with Sérsic's (1966) law,  $\rho(R) = a e^{-b[(R/R_C)^{1/m} - 1]}$ . Since it is rather insensitive to variations of  $R_C$ , we used the same core-like radius as that indicated by the composed power-law in order to have less free parameters when fitting Sérsic's law. The best fit was obtained with  $n = 4.1 \pm 0.7$  and  $CC = 0.88$ .

#### 4.2. Metal-rich GCs

The 33 metal-rich GCs of RS-GC05 are contained in the region  $0.66 \leq R_{GC}(\text{kpc}) \leq 8.3$  (panel b), which shows that a sharp radial cutoff thus occurs in the metal-rich distribution near the Solar circle. Metal-rich GCs in GC05 located outside this region appear to be related to accretion of dwarfs and/or young ages (Table 1). This contrasts with the metal-poor GCs that distribute in the range  $0.36 \leq R_{GC}(\text{kpc}) \leq 123$ . Similar to the metal-poor GCs, a flattening in the radial distribution of the metal-rich GCs with respect to the extrapolation of the large Galactocentric distance power-law  $\sim R^{-(3.2 \pm 0.2)}$  occurs for  $R_{GC} \leq 2 \text{ kpc}$ . This effect should be expected, since there is a lack of correlation of metallicity and GC luminosity (e.g. Djorgovski & Meylan 1994; van den Bergh 2003). Parameters of the composed power-law fit are  $\rho_0 = 6.3 \pm 5.2 \text{ kpc}^{-3}$ ,  $R_C = 1.2 \pm 1.0 \text{ kpc}$  and  $\alpha = 3.9 \pm 1.2$ , with  $CC = 0.88$ . Sérsic's law (inset of panel b) provides a fit with the exponent  $n = 2.9 \pm 1.5$  ( $CC = 0.87$ ). In this fit we used  $R_C = 1.2 \pm 1.0 \text{ kpc}$ , as indicated by the composed power-law. The observed distribution (panel b of Fig. 5) cannot be fitted with an exponential-decay law, which precludes the presence of a disk.

Probably as a consequence of the bulge/halo transition, the flattening in both metal-poor and metal-rich radial distributions begin at Galactocentric distances compatible with the dimension of the bulge (Sect. 3), particularly with the  $(x, y, z)$  scale-lengths of the metal-rich GCs (Table 2).

Despite the marked difference in the radial extent of the metal-rich and metal-poor GC profiles, both distributions present similar structural features such as flattening in the central region, core-like radius ( $R_C = 1.2\text{--}1.5 \text{ kpc}$ ), composed ( $\alpha = 3.9$ ) and single power-law slopes ( $n = 3.2\text{--}3.5$ ) and Sérsic's law index ( $n = 2.9\text{--}4.1$ ), within uncertainties. These similarities suggest that most of the GCs in both metallicity classes share a common origin.

#### 4.3. All GCs of the reduced sample

The best-fit of the composed power-law to the radial distribution of the 116 RS-GC05 GCs was obtained with  $\rho_0 = 7.2 \pm 3.0 \text{ kpc}^{-3}$ ,  $R_C = 1.9 \pm 0.5 \text{ kpc}$ , and  $\alpha = 4.4 \pm 0.3$ , with  $CC = 0.91$  (panel c of Fig. 5). Because the metal-rich GCs are contained in the region  $R_{GC}(\text{kpc}) \leq 8.3$ , the slope of the composed power-law was slightly steeper than those of the metal-rich and metal-poor distributions, as expected. In addition, the single power-law extrapolation for  $R_{GC} \geq 3.5 \text{ kpc}$  falls off as  $\sim R^{-(3.9 \pm 0.1)}$ , which basically agrees within uncertainties with that of the metal-poor GCs. The best Sérsic's law fit was obtained with  $n = 3.0 \pm 0.4$  and  $CC = 0.89$ . Qualitatively, Sérsic's law and the composed power-law basically provide the same fit to the observed radial profile.

#### 4.4. Spherically symmetric-volume densities for the oblate metal-rich sub-system

For practical purposes we assumed spherical symmetry in the above analysis of metal-rich and metal-poor radial density profiles. However, the metal-rich GCs distribute through a region whose geometry is clearly oblate (Sect. 3). Thus, spherically symmetric-volume densities calculated in radial bins beyond a few kpc from the centre will be artificially decreased, as compared to those measured in a genuinely (or approximately) spherical system. Consequently, both the measured power-law fall-off at large radii and central flattening degree in the metal-rich sub-system might be enhanced relative to the nearly spherically symmetric metal-poor sub-system.

To investigate the effects of non-sphericity in the metal-rich sub-system we applied a coordinate transformation to correct for its oblateness,  $y \rightarrow y/0.9$  and  $z \rightarrow z/0.4$  (Sect. 3). Subsequently we recalculated Galactocentric distances,  $R_{GC} = \sqrt{x^2 + y^2 + z^2}$ , and volume densities,  $\rho(R)$ . Compared to the observed oblate profile (bottom panel), the corrected one (top panel of Fig. 6) presents a similar shape and somewhat scaled-up Galactocentric distances. The fit of the composed power-law results in a core-like  $R_C = 0.9 \pm 0.9 \text{ kpc}$  and slope  $\alpha = 3.2 \pm 0.9$ . Both  $R_C$  and  $\alpha$  are similar to the previous ones, but the slope is somewhat flatter, as expected.

We conclude within uncertainties that measuring spherically symmetric volume densities in the oblate metal-rich GC sub-system has a small effect on structural parameters, such as power-law fall-off at large radii and flattening degree in the central region. The effect is minimal probably because of the relatively small radial extension ( $R_{GC} \sim 10 \text{ kpc}$ ) of the metal-rich sub-system. This effect is negligible for the nearly-spherical metal-poor GC sub-system (Sect. 3).

#### 4.5. Globular cluster destruction rates

The discussions in the previous section raised the question whether the flattening observed in the radial distribution for regions interior to  $R_{GC} \sim 2 \text{ kpc}$  is a primordial feature or a consequence of enhanced GC-destruction rates near the Galactic centre. Although the present analysis does not answer this

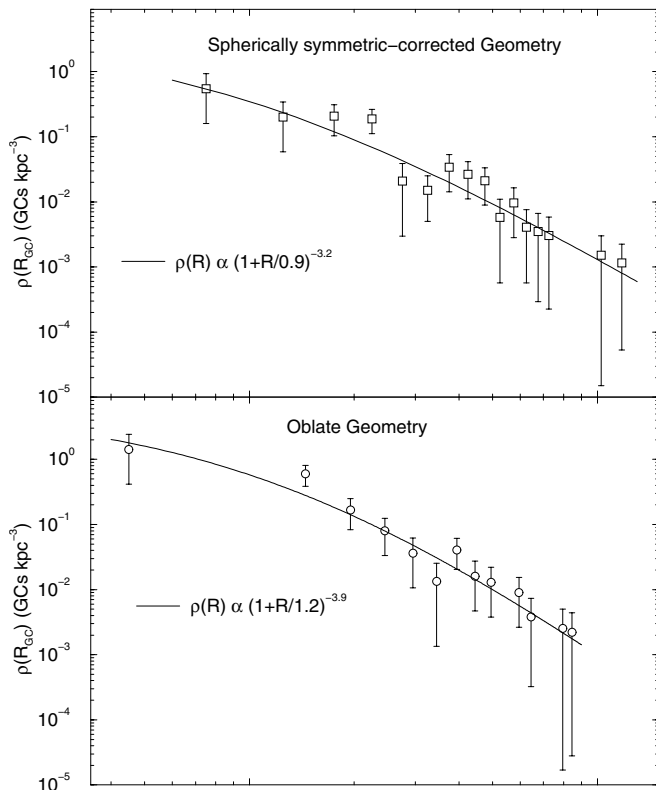


**Fig. 6.** Radial density profiles of the metal-rich GCs in the reduced sample measured with spherically symmetric volume densities on oblateness-corrected (*top panel*) and oblate (*bottom panel*) spatial geometries.

question, it can be used to provide an estimate on the fraction of primordial GCs still present in the Galaxy.

The Galactic environment, particularly near the centre, tends to destroy star clusters because of enhanced tidal truncation and gravitational shocks due to passages close to the bulge and through the disk. The bulge, in particular, is very efficient in destroying clusters on highly elongated orbits (Gnedin & Ostriker 1997), and the presence of the bar increases the destruction rates by providing a means to bring more clusters close to the Galactic centre (Long et al. 1992). Dynamical evaporation is probably the most important destruction mechanism in the present-day Galactic environment (Gnedin & Ostriker 1997). Aguilar et al. (1988) estimate a current GC depletion rate of  $\sim 5\%$  due basically to dynamical evaporation, indicating that most of the destruction took place in the past with bulge-shocking as the main factor. Hut & Djorgovski (1992) estimate that the present GC evaporation rate may be  $5 \pm 3 \text{ Gyr}^{-1}$ .

Gnedin & Ostriker (1997) found larger destruction rates than did previous works, predicting that  $52\%–86\%$  of the present GC population may be destroyed in the next Hubble time. They conclude that the present GC population must be a small fraction of the primordial one, with the debris of the destroyed clusters constituting a large fraction of the spheroidal (bulge + halo) stellar population. Mackey & van den Bergh (2005) estimate that the present population could be a fraction  $\sim 2/3$  of the original one by means of observational differences in properties of three Galactic GC subsystems.

Mackey & Gilmore (2004) estimate a lower limit of  $50\%$  for the destruction rate over the last Hubble time, an intermediate value between those of Gnedin & Ostriker (1997) and Mackey & van den Bergh (2005).

At large Galactocentric distances the efficiency of the GC destruction mechanisms should be minimised with respect to the central region. This assumption is supported by numerical simulations showing that low-concentration, high-mass GCs are efficiently destroyed in the inner halo but are able to survive at  $R_{GC} \geq 10 \text{ kpc}$  (Vesperini & Heggie 1997). For large  $R_{GC}$  the number-density of GCs in RS-GC05 is described well by the single power-law  $\rho(R) = (14.2 \pm 3.3)R^{-(3.9 \pm 0.1)}$ , the discrepancy with respect to the observed profile becoming increasingly larger for  $R_{GC} \leq 3 \text{ kpc}$  (Fig. 5 – panel c).

An estimate of the past destruction rate can be derived by comparing the number of GCs in RS-GC05 with one corresponding to the extrapolation of the large- $R_{GC}$  power-law to the inner regions, under the assumption that the difference in both numbers is basically due to the cumulative past destruction of GCs. This estimate should be taken as a lower-limit, since we neglect GC destruction for large  $R_{GC}$ . To derive this value we integrate the large- $R_{GC}$  power-law through the Galactocentric distance range over which the 116 GCs of RS-GC05 are observed. Taking the uncertainties in the parameters of the power-law fit into account, we estimate that the present GC population represents the fraction  $\leq 23 \pm 6\%$  of the primordial one. Thus, a lower-limit for the past destruction rate is  $\sim 77\%$  over a Hubble time. This estimate is compatible with the one in Gnedin & Ostriker (1997) and about three times higher than was derived by Mackey & van den Bergh (2005).

The above estimate is based on the assumption that the flattening in the central radial profile is essentially due to GC destruction. However, if the flattening is partly primordial, as suggested by Parmentier & Grebel (2005), the  $\sim 77\%$  destruction rate should in fact be taken as an approximate upper limit. In this case our estimate would agree with the central range of Gnedin & Ostriker (1997).

#### 4.6. The central kpc

With the present determination of the Galactocentric distance (Sect. 3.1), 9 GCs of the reduced sample are located within 1 kpc of the Galactic centre (H03 contains 11 such GCs). The metal-poor GCs are Palomar 6 and HP 1 at  $R_{GC} \leq 0.5 \text{ kpc}$ , and NGC 6355, Terzan 9, NGC 6522, NGC 6558, and NGC 6401 at  $0.5 \leq R_{GC}(\text{kpc}) \leq 1.0$ . The metal-rich ones are Terzan 5 and ESO 456 SC38 at  $0.6 \leq R_{GC}(\text{kpc}) \leq 0.7$ . Errors affect these individual estimates, but the ensemble might give hints to the extent of a potential avoidance zone or to a central region of enhanced destruction rates (e.g. Aguilar et al. 1988).

## 5. Discussion

In the analysis of the reduced sample GCs we found that the radial density profiles of the metal-rich and metal-poor GCs are described well by a composed power-law of the form  $\rho(R) \propto (1 + R/R_C)^{-\alpha}$  with  $3.9 \leq \alpha \leq 4.4$ . For Galactocentric distances larger than  $\sim 2 \text{ kpc}$ , both observed profiles fall off as a single



power-law  $R^{-n}$  with  $3.2 \leq n \leq 3.9$ , while for inner regions they both flatten in a similar way. Structurally, the only difference besides geometry (Sect. 3) between the spatial distributions of the metal-rich and metal-poor GCs is that the former basically extends to the Solar circle, while the latter spans from the central parts to the outer halo. This suggests that a significant fraction of the metal-rich and metal-poor GCs share a common origin. These conclusions are not significantly affected by the oblate and nearly spherical geometries of the metal-rich and metal-poor sub-systems, respectively (Sect. 4.4).

As pointed out by Djorgovski & Meylan (1994), the analytical function that we adopted to fit the radial density profiles does not have a physically consistent counterpart. However, the steep slopes implied by this function for the GC radial density profiles rule out scenarios involving the pure monolithic collapse of an isothermal, uniform density cloud. This kind of collapse would produce flatter radial density profiles (Abadi et al. 2006, and references therein). In addition, RS-GC05 radial density slopes are significantly steeper than for the dark matter halo (Merritt et al. 2005), which in principle precludes a common origin of these structures. Consequently, additional mechanisms might have been necessary to increase the density of GCs in the central regions of the Milky Way, such as mergers in the early phases.

The rather steep density distribution of the stellar halo was previously derived using globular clusters, RR Lyrae stars, blue horizontal-branch (BHB) stars, and star counts. Harris (1976) and Zinn (1985) have shown that the metal-poor GCs distribute radially following a  $R^{-n}$  power-law profile, with  $n = 3.5$ . Using observations of RR Lyrae Hawkins (1984) derived  $n = 3.1$  with an axial ratio  $c/a = 0.9$ . Bahcall & Soneira (1984) and Gilmore (1984) found  $c/a \approx 0.8$ . Using BHB stars Preston et al. (1991) found an increase in the axial ratio from  $c/a \approx 0.5$  to  $c/a \approx 1$  up to 20 kpc with  $n = 3.5$ . Recently, Yanny et al. (2000) used BHB tracers from Sloan Digital Sky Survey data to derive  $c/a = 0.65$  and  $n = 3.2$ . Ivezić et al. (2000) found that the RR Lyrae column density follows a shallower power law with  $n = 2.7$ . Robin et al. (2000) from deep wide-field star counts estimated a halo flattening of 0.76, and  $n = 2.44$ .

Evidence of merger events in galaxies has considerably increased in recent years, both on observational and theoretical grounds. Deep observations of stars in luminous halos associated with numerical simulations of galaxy formation in  $\Lambda$ -cold dark matter ( $\Lambda$ CDM) scenarios indicate that a large fraction of the stellar content in the halo was not formed in situ. Abadi et al. (2006 and references therein) suggest that this fraction may have been accreted from protogalaxies during earlier merger events. The resulting mass density profiles behave as a power-law  $R^{-n}$  with  $n = 3$  at the luminous edge of the galaxy and  $n \geq 4$  more externally, at the virial radius. In addition, the density profile of the outer stellar halo is more centrally concentrated with a steeper slope than the dark matter halo, whose density profile is characterised by slopes  $n = 1-3$  (Merritt et al. 2005). Hierarchical galaxy formation models in the  $\Lambda$ CDM framework that are successful in reproducing the radial density profile of the Milky Way stellar halo indicate that this structure formed from  $\sim 100$  tidally disrupted, accreted dwarf satellites (Bullock et al. 2001). What emerges from this is an

observational/theoretical picture of the formation and evolution of the stellar halo involving violent relaxation and accretion, one that is consistent with hierarchical models of galaxy formation (Bellazzini et al. 2003; Abadi et al. 2006).

In this sense, the observed similarity between the metal-rich and metal-poor radial density profiles of the Galactic GC system and that of the stellar halo suggests that, in addition to the GCs formed in the primordial collapse, a non-negligible fraction of the GCs presently in the Milky Way was probably accreted during an early period of active merging. This scenario seems to apply to the bulge as well, which raises the possibility of an early merger affecting the central parts of the Galaxy. In the present universe there are examples of such mergers, e.g. NGC 1275 (Zepf et al. 1995; Holtzman et al. 1992).

Additional support for this scenario comes from the fact that the radial density profiles of the GCs of the reduced sample are equally well fitted by Sérsic's law,  $\rho(R) \propto e^{-b[(R/R_c)^{1/n}-1]}$ , with  $n \approx 4.1$  (metal-poor),  $n \approx 2.9$  (metal-rich), and  $n \approx 3.0$  (combined metal-poor/metal-rich GCs). Sérsic's law with  $2 \leq n \leq 4$  is thought to apply to systems resulting from the mixing that follows from violent relaxation or merging (Merritt et al. 2005, and references therein). Besides, chemical evolution models that reproduce the observed abundances of stars in the bulge suggest that the Galactic bulge formed from the same gas but faster than the inner Galactic halo (Matteucci & Romano 1999; Matteucci et al. 1999). The minimum at about  $[\text{Fe}/\text{H}] \approx -0.75$  in the observed metallicity distribution of GCs (Fig. 1) may reflect an external mechanism, such as merging, to explain the exceedingly large number of metal-rich GCs. An early merger in the Milky Way with a relatively massive galaxy might have provided the excess metal-rich star formation in the central parts.

Further evidence of the bulge formation via collapse and/or additional mechanisms will be given by detailed derivation of metallicities and abundance ratios in comprehensive samples of GCs. However, such detailed information for bulge GCs is presently scarce.

## 6. Concluding remarks

In this paper the Galactic globular cluster system was decontaminated of those objects with strong evidence of external origin and/or ages younger than the Galaxy collapse. The resulting reduced sample contains 116 GCs, 81 metal-poor and intermediate metallicity clusters ( $[\text{Fe}/\text{H}] \leq -0.75$ ), 33 metal-rich, and 2 with unknown metallicity. The classical bimodal metallicity distribution is enhanced in the reduced sample.

Projections of the observed heliocentric distances onto the  $(x, y, z)$  planes show that the metal-rich GCs distribute in a central region of dimensions  $\sim 12 \text{ kpc} \times 11 \text{ kpc} \times 5 \text{ kpc}$ , whose structure resembles an oblate spheroidal with axial ratio  $c/a \approx 0.4$ . The metal-poor ones span a region of dimensions  $\sim 35 \text{ kpc} \times 36 \text{ kpc} \times 30 \text{ kpc}$  with a shape that is similar to a slightly flattened sphere with  $c/a \approx 0.8$ . The metal-poor GCs in the reduced sample extend into the beginning of the outer halo. Based on the projected number-density of GCs along the  $x$ -direction, we measured the distance of the Sun to the Galactic centre as  $R_0 = 7.2 \pm 0.3 \text{ kpc}$ . This value was obtained by

considering the spatial distribution of 116 GCs and is  $\sim 10\%$  smaller than the widely used estimate of Reid (1993).

Based on structural similarities of the radial density profiles of the present-day GC population with the stellar halo, one can build a scenario where, besides the GCs formed in the primordial collapse, a non-negligible fraction of the Milky Way GCs was probably accreted from satellites during an early period of merging. Observational and theoretical evidence supports this picture; e.g. the GCs formed as a consequence of mergers in NGC 1275 (Zepf et al. 1995; Holtzman et al. 1992).

The present decontamination procedure was not sensitive to all accretions that may have occurred in the first Gyr of the Galaxy, including an eventual major merging, since the observed radial density profiles still appear to preserve traces of the earliest merger(s).

Assuming that the flattening in the observed radial density profiles is a consequence of the cumulative GC depletion mostly by bulge and disk shocking, we estimated that the present GC population represents a fraction that is  $\leq 23 \pm 6\%$  of the original one. This implies a lower-limit destruction rate of  $\sim 77\%$  over a Hubble time. This estimate is compatible with the one in Gnedin & Ostriker (1997) and somewhat larger than the one derived by Mackey & van den Bergh (2005). However, if the central flattening is partly primordial (Parmentier & Grebel 2005), our estimate would in fact be an upper limit.

The significant improvement in the accuracy of GC data over the past years, as analysed in the present work, has shed light on the issue of whether the metal-rich GCs are associated to a disk (e.g. Zinn 1985; Armandroff 1989) or to a spheroidal subsystem. The fact that the volume-density radial distribution of GCs of the reduced sample can be described both by a core-like power-law or a Sérsic's law indicates that the metal-rich GC subsystem is spheroidal.

The present study points out that, besides the GC accretions from dwarfs and/or formation later than the primordial collapse, the radial density distributions require a non-negligible early merger population, in addition to a primordial collapse component. This scenario also provides a natural explanation to the second peak in the bimodal metallicity distribution. Through gravitational lensing, large galaxies at high-redshift have been detected in the starburst stage, in an epoch compatible to that of the Milky Way's primordial collapse. Examples are the  $z \sim 7$  and  $M \sim 10^9 M_\odot$  galaxy lensed by the Abell 2218 cluster (Egami et al. 2005) and the  $z \sim 5.5$ ,  $M \sim 1-6 \times 10^{10} M_\odot$  starforming galaxy in the field of the cluster RDCS 1252.9-2927 (Dow-Hygelund et al. 2005). Collapse or its combination with merging are supported by the Galactic GCs and large redshift observations of galaxies. On the other hand, pure hierarchical galaxy formation has yet to be observed in detail.

*Acknowledgements.* E.B., C.B., and B.B. acknowledge support from the Brazilian Institution CNPq. S.O. acknowledges support from the Ministero dell'Università e della Ricerca Scientifica e Tecnologica (MURST) under the program on "Fasi Iniziali di Evoluzione dell'Alone e del Bulge Galattico" (Italy). We thank the anonymous referee for comments.

## References

- Abadi, M. G., Navarro, J. F., & Steinmetz, M. 2006, MNRAS, 365, 747
- Aguilar, L., Hut, P., & Ostriker, J. P. 1988, ApJ, 335, 720
- Armandroff, T. E. 1989, AJ, 97, 375
- Bahcall, J. N., & Soneira, R. M. 1984, ApJS, 55, 67
- Barbuy, B., Bica, E., & Ortolani, S. 1998, A&A, 333, 117
- Barbuy, B., Ortolani, S., Bica, E., & Desidera, S. 1999, AJ, 348, 783
- Bellazzini, M., Ferraro, F., & Ibata, R. 2003, AJ, 125, 188
- van den Bergh, S. 1993, AJ, 105, 971
- van den Bergh, S. 2000, in *The Galaxies of the Local Group*, (Cambridge: Cambridge University Press), UK, Cambridge, Astrophysics Ser., 35
- van den Bergh, S. 2003, ApJ, 590, 797
- Binney, J., & Tremaine, S. 1987, in *Galactic Dynamics* (Princeton, NJ: Princeton University Press), Princeton series in astrophysics
- Bullock, J. S., Kravtsov, A. V., & Weinberg, D. H. 2001, ApJ, 548, 33
- Carraro, G. 2005, ApJ, 621, 61
- da Costa, G. S., & Armandroff, T. E. 1995, AJ, 109, 2533
- Coté, P. 1999, AJ, 188, 406
- Coté, P., Welch, D. L., Fischer, P., & Gebhardt, K. 1995, ApJ, 454, 788
- Dinescu, D. I., Girard, T. M., & van Altena, W. F. 1999, AJ, 117, 1792
- Djorgovski, S., & Meylan, G. 1994, AJ, 108, 1292
- Dow-Hygelund, C. C., Holden, B. P., Bouwens, R. J., et al. 2005, ApJ, 630, L137
- Ducati, J. R., Ribeiro, D., & Rembold, S. B. 2003, ApJ, 588, 344
- Dutra, C. M., & Bica, E. 2000, A&A, 359, 9
- Egami, E., Kneib, J.-P., Rieke, G. H., et al. 2005, ApJ, 618, L5
- Eggen, O. J., Lynden-Bell, D., & Sandage, A. R. 1962, ApJ, 136, 748
- Eisenhauer, F., Schödel, R., Genzel, R., et al. 2003, ApJ, 597, L121
- Forbes, D. A., Strader, J., & Brodie, J. P. 2004, AJ, 127, 3394
- Frenk, C. S., & White, S. D. M. 1982, MNRAS, 198, 173
- Gilmore, G. 1984, MNRAS, 207, 223
- Gnedin, O. Y., & Ostriker, J. P. 1997, ApJ, 474, 223
- Grebel, A. K., & Roberts, W. 1995, A&AS, 109, 293
- Guo, X., Girard, T. M., van Altena, W. F., & Lopez, C. E. 1993, AJ, 105, 2182
- Harris, W. E. 1976, AJ, 81, 1095
- Harris, W. E. 1996, AJ, 112, 1487
- Harris, W. E., Phelps, R. L., Madore, B. F., Pevunova, O., & Skiff, B. A. 1997, AJ, 113, 688
- Hawkins, M. R. S. 1984, MNRAS, 206, 433
- Holtzman, J. A., Faber, S. M., Shaya, E. J., et al. 1992, AJ, 103, 691
- Hurt, R. L., Jarrett, T. H., Kirkpatrick, J. D., et al. 2000, AJ, 120, 1876
- Hut, P., & Djorgovski, S. 1992, Nature, 359, 806
- Ibata, R. A., Irwin, M. J., & Gilmore, G. 1994, Nature, 370, 194
- Ibata, R. A., Wyse, R. F. G., Gilmore, G., Irwin, M. J., & Suntzeff, N. B. 1997, AJ, 113, 634
- Ivezić, Z., Goldston, J., Finlator, K., et al. 2000, AJ, 120, 963
- Kinman, T. D. 1959, MNRAS, 119, 538
- Kobulnicky, H. A., Monson, A. J., Bickalew, B. A., et al. 2005, AJ, 129, 239
- van der Kruit, P. C., & Searle, L. 1981, A&A, 105, 115
- Long, K., Ostriker, J. P., & Aguilar, L. 1992, ApJ, 388, 362
- Maciel, W. J. 1993, Ap&SS, 206, 285
- Mackey, A. D., & Gilmore, G. F. 2004, MNRAS, 355, 504
- Mackey, A. D., & van den Bergh, S. 2005, MNRAS, 360, 631
- Matteucci, F., & Romano, D. 1999, Ap&SS, 265, 311
- Matteucci, F., Romano, D., & Molaro, P. 1999, A&A, 341, 458
- Merritt, D., Navarro, J., Ludlow, A., & Jenkins, A. 2005, ApJ, 624, L85
- Minniti, D. 1995, AJ, 109, 1663

- Olson, B. I. 1975, *PASP*, 87, 349
- Ortolani, S., Bica, E., & Barbuy, B. 2000, *A&A*, 361, L57
- Parmentier, G., & Grebel, E. K. 2005, *MNRAS*, 359, 615
- Phelps, R. L., & Schick, M. 2003, *AJ*, 126, 265
- Preston, G. W., Shectman, S. A., & Beers, T. C. 1991, *ApJ*, 375, 121
- Rastorguev, A. S., Pavlovskaya, E. D., Durlevich, O. V., & Filippova, A. A. 1994, *AstL*, 20, 591
- Reid, M. J. 1993, *ARA&A*, 31, 345
- Rice, W., Merrill, K. M., Gatley, I., & Gillett, F. C. 1996, *AJ*, 112, 114
- Robin, A. C., Reyl , C., & Cr z , M. 2000, *A&A*, 359, 103
- Rosenberg, A., Saviane, I., Piotto, G., & Aparicio, A. 1999, *AJ*, 118, 2306
- Salaris, M., & Weiss, A. 2002, *A&A*, 388, 492
- Sandage, A. 1990, *JRASC*, 84, 70
- Schlegel, D. J., Finkbeiner, D. P., & Davis, M. 1998, *ApJ*, 500, 525
- Searle, L., & Zinn, R. 1978, *ApJ*, 225, 357
- S rsic, J. L. 1966, in *Atlas de Galaxias Australes*; Observatorio Astronomico de C rdoba, 141
- Siegel, M. H., Majewski, S. R., Cudworth, K. M., & Takamiya, M. 2001, *AJ*, 121, 935
- Sumi, T. 2004, *MNRAS*, 349, 193
- Vesperini, E., & Heggie, D. C. 1997, *MNRAS*, 289, 898
- Willman, B., Blanton, M. R., West, A. A., et al. 2005, *AJ*, 129, 2692
- Yanny, B., Newberg, H. J., Kent, S., et al. 2000, *ApJ*, 540, 825
- Zepf, S. E., Carter, D., Sharples, R. M., & Ashman, K. 1995, *ApJ*, 445, L19
- Zinn, R. 1980, *ApJ*, 241, 602
- Zinn, R. 1985, *ApJ*, 293, 424
- Zinn, R. 1993, in *The Globular Cluster-Galaxy Connection*, ed. G. H. Smith, & J. P. Brodie, *ASP Conf. Ser.*, 48 (San Francisco: ASP), 38